Immunoglobulin G (IgG) Fab Glycosylation Analysis Using a New Mass Spectrometric High-throughput Profiling Method Reveals Pregnancy-associated Changes*[S]

Albert Bondt‡§, Yoann Rombouts§¶, Maurice H. J. Selman§, Paul J. Hensbergen§, Karli R. Reiding§, Johanna M. W. Hazes‡, Radboud J. E. M. Dolhain‡, and Manfred Wuhrer§‖‡‡**

The *N*-linked glycosylation of the constant fragment (Fc) of immunoglobulin G has been shown to change during pathological and physiological events and to strongly influence antibody inflammatory properties. In contrast, little is known about Fab-linked N-glycosylation, carried by ~20% of IgG. Here we present a high-throughput workflow to analyze Fab and Fc glycosylation of polyclonal IgG purified from 5 μl of serum. We were able to detect and quantify 37 different N-glycans by means of MALDI-TOF-MS analysis in reflectron positive mode using a novel linkage-specific derivatization of sialic acid. This method was applied to 174 samples of a pregnancy cohort to reveal Fab glycosylation features and their change with pregnancy. Data analysis revealed marked differences between Fab and Fc glycosylation, especially in the levels of galactosylation and sialylation, incidence of bisecting GlcNAc, and presence of high mannose structures, which were all higher in the Fab portion than the Fc, whereas Fc showed higher levels of fucosylation. Additionally, we observed several changes during pregnancy and after delivery. Fab N-glycan sialylation was increased and bisection was decreased relative to postpartum time points, and nearly complete galactosylation of Fab glycans was observed throughout. Fc glycosylation changes were similar to results described before, with increased galactosylation and sialylation and decreased bisection during pregnancy. We expect that the parallel analysis of IgG Fab and Fc, as set up in this paper, will be important for unraveling roles of these glycans in (auto)immunity, which may be mediated via recognition by human lectins or modulation of antigen binding. ***Molecular & Cellular Proteomics 13: 10.1074/mcp.M114.039537, 3029–3039, 2014.***

Immunoglobulins are key players of the human immune system. Immunoglobulin G (IgG)[1] is the most abundant representative of this group, with serum concentrations of ~10 mg/ml (1). It consists of two heavy chains (γ-chains) made up of three constant regions (C_H1, C_H2, and C_H3) and one variable region (V_H). Attached to each heavy chain is a light chain (λ or κ). Based on chemical and biological properties, different regions can be distinguished in the IgG molecule: two antigen binding fragments (obtained as $F(ab')_2$ by IdeS treatment; herein referred to as Fab) and a crystallizable fragment (Fc). The structure of IgG is schematically presented in Fig. 1.

IgGs are glycoproteins, and N-glycans are present at Asn297 of the C_H2 domain. These glycans consist of a constant heptasaccharide core that is often modified by a core fucose and is in part decorated with bisecting N-acetylglucosamine (GlcNAc), galactose(s), and sialic acid(s) (Fig. 1) (1). The Fc glycans have been extensively studied, and glycosylation changes have been found to be associated with disease (*e.g.* rheumatoid arthritis) (2, 3) and aging (4–6). Several immune regulatory properties have been demonstrated for IgG Fc glycans (7–13). For example, Fc-linked glycans influence the IgG effector function by altering the three-dimensional structure of the protein, and thereby the binding to Fcγ-receptors (12, 13). Additionally, glycan–glycan interactions occur between IgG and Fcγ-recep-

From the ‡Department of Rheumatology, Erasmus University Medical Center, 3000 CA Rotterdam, The Netherlands; §Center for Proteomics and Metabolomics, Leiden University Medical Center, Albinusdreef 2, 2333 ZA Leiden, The Netherlands; ¶Department of Rheumatology, Leiden University Medical Center, Albinusdreef 2, 2333 ZA Leiden, The Netherlands; ‖Division of BioAnalytical Chemistry, VU University Amsterdam, 1081 HV Amsterdam, The Netherlands; **Department of Molecular Cell Biology and Immunology, VU University Medical Center, 1007 MB Amsterdam, The Netherlands

⌘ *Author's Choice*—Final version full access.

Received March 18, 2014, and in revised form, June 4, 2014

Published, MCP Papers in Press, July 8, 2014, DOI 10.1074/mcp.M114.039537

Author contributions: A.B., Y.R., M.H.S., P.J.H., J.M.H., R.J.D., and M.W. designed research; A.B. performed research; A.B. and K.R.R. contributed new reagents or analytic tools; A.B., R.J.D., and M.W. analyzed data; A.B., Y.R., M.H.S., P.J.H., K.R.R., R.J.D., and M.W. wrote the paper.

[1] The abbreviations used are: IgG, immunoglobulin G; ACN, acetonitrile; ConA, concanavalin A; Fab, antigen binding fragment; Fc, crystallizable fragment; GlcNAc, N-acetylglucosamine; HILIC, hydrophilic interaction liquid chromatography; SPE, solid phase extraction.

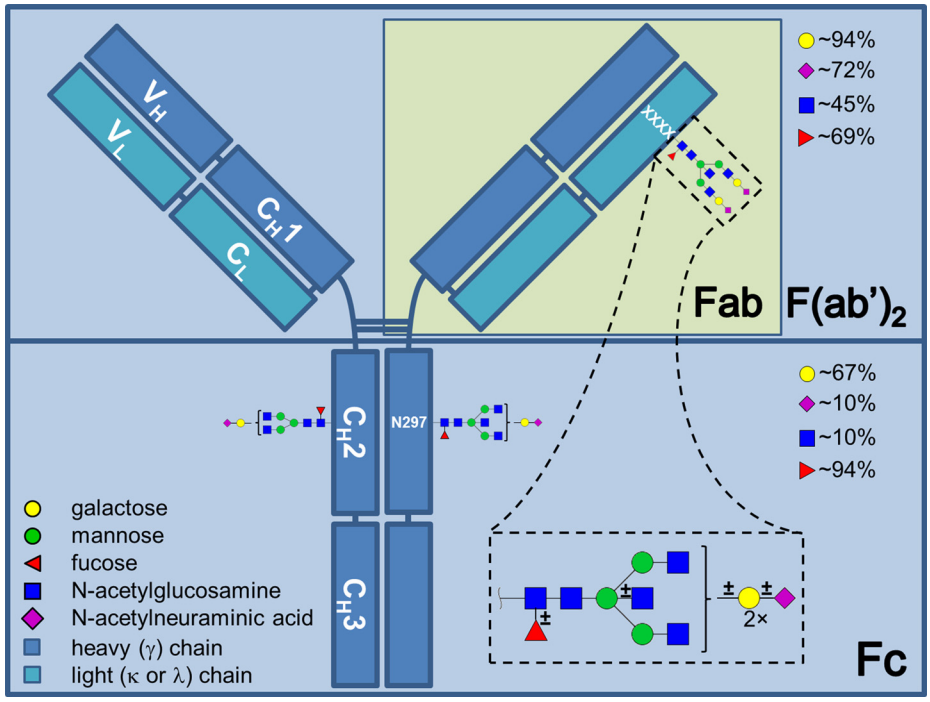

FIG. 1. **Schematic representation of IgG with the heavy γ chains (dark blue), light chains (lighter blue), and N-glycans.** In the top right-hand corner of the Fc and Fab areas, the percentages of galactosylation, sialylation, bisection, and fucosylation are depicted. The inset represents the stable heptasaccharide core with possible extensions.

tor-IIIa (8), with the presence of a core fucose decreasing this affinity by ~2 orders of magnitude (7).

The Fab portion consists of the heavy chain C_H1 and V_H regions combined with a light chain and exhibits the antigen binding sites formed by the variable and hypervariable regions of those two chains. N-glycans are known to occur on 15% to 25% of the IgG Fab portions (1, 14, 15). The Fab N-glycans can be involved in immunomodulation, because they influence the affinity and avidity of antibodies for antigens (16–19), as well as antibody half-life (17, 20). The glycans of the Fab have been described as biantennary complex-type structures that are, in contrast to Fc glycans, highly sialylated (21–23). Additionally, high-mannose-type structures have been said to be located on the Fab portion (23).

Pregnancy is known to be associated with overall changes in IgG glycosylation. Indeed, a marked increase of galactosylation and sialylation has been observed in IgG Fc glycosylation during pregnancy (3, 24, 25). In addition, lectin binding studies suggest changes in Fab glycosylation of IgG during pregnancy (26), which may be caused by increased levels of progesterone (27). Changes in glycosylation during pregnancy could be one of the mechanisms that contribute to acceptance of the fetal allograft by the maternal immune system (26).

Our knowledge on the Fab glycosylation of IgGs from peripheral blood is scarce, which is in part due to difficulty detecting the glycans in a Fab-region-specific manner. Because of the polyclonal nature of serum IgG, one may expect Fab glycans to be attached to a large variety of sequence motifs arising from somatic rearrangements and mutations (28), making the analysis of Fab glycopeptides from polyclonal serum IgG very demanding, if feasible at all. Therefore, study of the Fab glycosylation of polyclonal serum IgG has mainly been pursued at the level of released glycans (14, 23). Difficulties lie in the purification of IgG and the separation of Fc and Fab glycosylation, which is essential for the assignment of the glycans to either part of the IgG molecule.

Here we present a high-throughput method for studying Fab glycosylation at the level of released glycans obtained from serum-derived polyclonal IgG. Using state-of-the-art affinity capturing beads and enzymes, we were able to obtain Fab and Fc separately, which, after glycan release, resulted in Fc- and Fab-specific glycan pools. The released glycans were subjected to a novel derivatization protocol resulting in linkage-specific modification of sialic acids, followed by HILIC sample purification and MALDI-TOF-MS. Finally, because marked changes in glycosylation during pregnancy have been described, the technique was applied to consecutive serum samples from a cohort of pregnant women. This approach was chosen to determine the usefulness of this technique in a clinical setting. The method proved to be able to demonstrate pregnancy-related changes in glycosylation of the Fab portion, in addition to the already known changes in Fc glycosylation (3, 24, 25).

EXPERIMENTAL PROCEDURES

Chemicals Used—Ethanol, trifluoroacetic acid (TFA), sodium dodecyl sulfate (SDS), disodium hydrogen phosphate dihydrate ($Na_2HPO_4 \times 2H_2O$), hydrochloric acid (HCl), and sodium chloride (NaCl) were purchased from Merck (Darmstadt, Germany). Hydroxybenzotriazole hydrate, 50% sodium hydroxide (NaOH), and Nonidet P-40 were obtained from Sigma-Aldrich. 1-ethyl-3-(3-dimethylaminopropyl)carbodiimide hydrochloride originated from Fluorochem (Hadfield, UK). Peptide:N-glycosidase F was bought from Roche Diagnos-

tics (Mannheim, Germany), 2,5-dihydroxybenzoic acid from Bruker Daltonics (Bremen, Germany), and HPLC SupraGradient ACN from Biosolve (Valkenswaard, The Netherlands). Milli-Q deionized water ($R > 18.2$ MΩ cm^{-1}; Millipore Q-Gard 2 system, Millipore, Amsterdam, The Netherlands) was used in this study.

IgG Purification—IgG was captured from 5 μl of serum. The serum is dilluted in 100 uL PBS. Using 10 μl of CaptureSelect IgG-Fc (Hu) beads (Invitrogen Europe, Bleiswijk, The Netherlands) in a 96-well format on an Orochem filter plate (10-μm pore size; Orochem Technologies, Naperville, IL). Alternatively CaptureSelect IgG-CH1 beads (Invitrogen Europe) or Protein G-Sepharose Fast Flow beads (GE Healthcare, Uppsala, Sweden) were used. The beads were washed three times with 200 μl of PBS on a vacuum manifold before the serum was applied to the beads. Application of the samples to the beads was followed by a 60-min shaking step at room temperature on a multiwell plate shaker with a 1.5-mm orbit at 1000 rpm (VWR, Amsterdam, The Netherlands). After removal of the diluted serum, the beads were washed twice with PBS and twice with digestion buffer (50 mM NaH_2PO_4/150 mM NaCl; pH 6.6).

On-bead FabRICATOR Digestion—IgG was specifically cleaved into Fc and Fab portions by recombinant streptococcal IdeS enzyme (tradename FabRICATOR; Genovis, Lund, Sweden) (29). The supplier's protocol was adjusted to simplify our procedure and reduce costs. We used 10 U of enzyme per 50 μg sample (IgG captured from 5 μl of serum, assuming an IgG serum concentration of 10 mg/ml), as compared with 50 U for 50 μg suggested by the supplier. To each sample, 35 μl of digestion buffer was added, containing 10 U of the enzyme. The Fc portions remained attached to the beads, and the flowthrough, containing Fab fragments, was collected via centrifugation (1 min, 50 × *g*) into V-bottom plates (Greiner Bio-One, Frickenhausen, Germany) after overnight incubation at 37 °C in a humidified environment. Following the washing steps with 3 × 200 μl of PBS and 3 × 200 μl of Milli-Q deionized water, the Fc portions were eluted using 100 μl of 100 mM HCl and collected into V-bottom plates containing 20 μl of 500 mM NaOH to neutralize the elution liquid and prevent the loss of sialic acids due to the acidic environment. Subsequently, both Fc and Fab samples were dried by vacuum centrifugation.

LC-MS/MS Analysis of IgG, Fc, and Fab Samples—To further investigate the sample purity, we performed proteomics analysis on the Fab-containing flowthrough and Fc- or IgG-containing eluates. The samples were dried in the vacuum centrifuge and reconstituted in 40 μl of 25 mM ammonium bicarbonate with 1 μl of 200 mM DTT. After 1 h of reduction at 60 °C, alkylation was performed with 3 μl of 220 mM iodoacetamide, followed by quenching with DTT and overnight digestion with trypsin (1:50 enzyme:protein ratio). LC–ion trap MS/MS analysis was performed as described previously (30). Peak lists were generated using Data Analysis 4.0 (Bruker Daltonics) with default settings and exported as Mascot generic files. Peptides were identified in the UniProt human 20131211 database (88,473 sequences; 35,069,569 residues) using the Mascot algorithm (Mascot 2.4.1, Matrix Science, London, UK), applying a combined search in Mascot Deamon 2.2.2. A peptide mass tolerance of ±0.5 Da (with the number of $^{13}C = 1$) and an MS/MS fragment tolerance of ±0.5 Da were used. Trypsin was designated as the enzyme, and up to one missed cleavage was allowed. Carbamidomethylcysteine was selected as a fixed modification, and oxidation of methionine as a variable modification. Proteins were considered truly detected when hits with at least two unique peptides with a score above 30 were observed.

N-glycan Release and Sialic Acid Ethyl Esterification—To release the N-glycans from both Fc and Fab, 10 μl of PBS and 20 μl of 2% SDS were added to the dried samples, which then underwent a 15-min incubation at 60 °C. Peptide:N-glycosidase F (0.25 U per sample) was added in 20 μl of a 5× PBS/4% Nonidet P-40 (1:1) solution, and the samples were incubated overnight at 37 °C in a desiccator.

The following day, 20 μl of the sample was added to 100 μl of 250 mM 1-ethyl-3-(3-dimethylaminopropyl)carbodiimide/250 mM hydroxybenzotriazole in pure ethanol. Ethyl esterification of sialic acids was performed at 37 °C for 1 h, as described before (31).

HILIC Purification of N-glycans—The ethyl esterified samples were prepared for cotton HILIC purification by the addition of 100 μl of ACN, followed by a 15-min incubation at −20 °C to precipitate proteins. As a modification of the original cotton HILIC micro-SPE method (32), a piece of cotton thread was used for glycan purification, as detailed in the following: for preparation of the HILIC micro-SPE devices, 20-μl pipette tips (Rainin Instrument, Oakland, CA) were packed with 3-mm cotton thread (180 μg, Pipoos, Utrecht, The Netherlands), which was then conditioned and equilibrated by pipetting 20 μl of Milli-Q deionized water three times and then 20 μl of 85% ACN three times. The sample was then loaded on the cotton by pipetting up and down 20 times. Finally, the cotton was washed three times with 20 μl of 85% ACN containing 1% TFA and three times with 20 μl of 85% ACN, followed by elution in 30 μl of Milli-Q deionized water.

MALDI-TOF-MS Measurement—One microliter of the glycan eluate was mixed on spot with 5 mg/ml 2,5-dihydroxybenzoic acid in 50% ACN containing 1 mM NaOH on a Bruker AnchorChip plate (part number 209514, 800-μm anchor; Bruker Daltonics) and allowed to dry at ambient temperature. Shortly before measurement, samples were recrystallized with 0.2 μl of EtOH. Measurement was performed using an UltrafleXtreme MALDI-TOF mass spectrometer (Bruker Daltonics) in reflectron positive mode. Automated measurement was performed in flexControl 3.4 Build 119. Random walk through the complete sample was used, with 20,000 shots per walk 200 shots per step at 2000 Hz. Summed spectra were saved.

Data Processing—The mass spectrometer was externally calibrated using peptide calibration mix (Bruker Daltonics). The obtained spectra were internally calibrated in flexAnalysis 3.3 Build 80 using a stepwise calibration with initial calibration on the following glycan species ($[M+Na]^+$): H3N4F1 (*m/z* 1485.534), H4N4F1 (*m/z* 1647.587), H4N5F1 (*m/z* 1850.666), H5N4E1 (*m/z* 1982.708), the second isotopic peak of H5N4F1E2 (*m/z* 2448.896), and the second isotopic peak of H5N5F1E2 (*m/z* 2651.975), with a 4 *m/z* peak picking window using the Snap algorithm. The initial calibration was followed by calibration on five different glycan peaks ($[M+Na]^+$) with a window of 1 *m/z*: H5N4 (*m/z* 1663.582), H5N4F1 (*m/z* 1809.640), H5N4F1E1 (*m/z* 2128.766), H5N4E2 (*m/z* 2301.835), and H5N5F1E1 (*m/z* 2331.845) (H, hexose; N, N-acetylhexosamine; F, fucose; E, ethyl esterified N-acetylneuraminic acid). These 11 calibrants cover the most abundant glycans of total IgG, Fc, and Fab glycan spectra. Calibrated spectra were exported as text files containing all data points with an *m/z* value and intensity. Internal calibration and export were performed using the flexAnalysis Batch Process (Bruker Daltonics). Using an in-house-developed script for Python (31), the spectrum was integrated at the *m/z* ranges that were calculated based on the theoretical glycan list of 42 theoretical N-glycan compositions. Processing in Python took about 4 s per spectrum. Output was saved as a text file that could be opened with Microsoft Excel 2010 for further analysis.

Of the 42 potential glycans, 37 N-glycan compositions were mostly observed with signal-to-noise ratios greater than 3 (supplemental Table S1). The relative abundance of the glycans was calculated after normalization to a total of 100%. For further analysis, the spectra had to pass a quality control set in Excel. Bad spectra were removed on the basis of cutoff criteria. More than 95% of the spectrum had to be explained by glycan peaks with a signal-to-noise ratio greater than 3. Additionally, the extracted data needed to have a total signal of >500,000 for all picked glycans after background subtraction. The

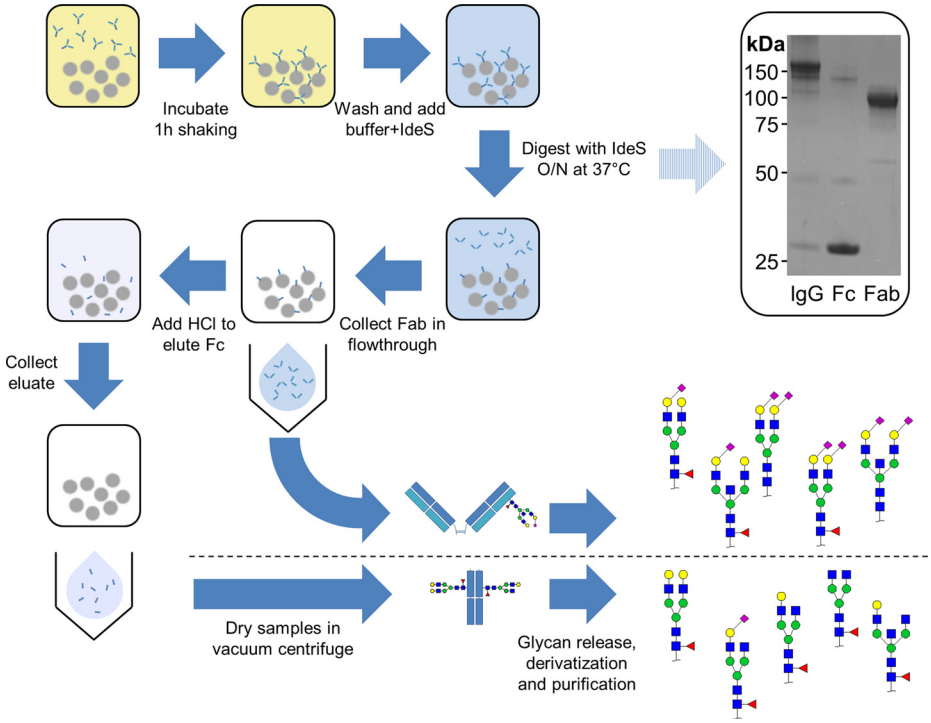

FIG. 2. **Workflow of IgG Fab and Fc glycosylation analysis, including an SDS-PAGE gel confirming IdeS digest.** IgG is captured from serum and digested overnight, and the flowthrough and eluate are collected. After drying, the glycans are released from the separate samples, derivatized, and purified before MALDI-TOF measurement.

glycan data were used to calculate global glycosylation traits: galactosylation; abundance of neutral, monosialylated, or disialylated glycans; fucosylation; bisection; abundance of high-mannose structures; or overall percentage of α2,3- and α2,6-linked sialic acids. The calculations are shown in the supplemental material. Of note, the sum of α2,3 and α2,6 sialic acids is not the same as the sum of monosialylated and disialylated glycans, as only one of two possible sialylation sites of monosialylated glycans contains a sialic acid.

Application to Clinical Samples—Sera from 29 healthy Caucasian women without adverse obstetric histories were obtained at three time points during pregnancy and three time points after delivery. The individuals participated as a reference group in the PARA (Pregnancy-induced Amelioration of Rheumatoid Arthritis) study (25). The study was in compliance with the Helsinki Declaration and was approved by the Ethics Review Board at the Erasmus University Medical Center, Rotterdam, The Netherlands. The last time point after delivery (range: 26–52 weeks postpartum) was added in a later stage of the study, and therefore the spread in weeks after delivery is larger than for the other time points, namely, 26–52 weeks. The above-described method was applied to 174 serum samples from the cohort, 9 standard serum samples, and 9 blanks. In total, 576 spectra were obtained. The relative abundance of the individual glycans and the calculated glycosylation traits were evaluated for these samples. Statistical analyses were performed using the "signrank" function in Stata/S.E. 13.0 for Windows (**StataCorp LP**, College Station, Texas). The Wilcoxon sign-ranked test was used to test pairwise differences between Fc and Fab glycans, Fc and Fab glycosylation traits, and changes within Fc or Fab glycosylation over time.

RESULTS

High-throughput Preparation of Polyclonal IgG Fab and Fc Portions—For the analysis of released N-glycans from IgG Fab and Fc, high protein purity has to be obtained. Additionally, Fab and Fc have to be separated properly. Here, we developed a high-throughput approach for the analysis of patient cohorts to get more insight into general principles in Fab glycosylation. The final approach presented here was obtained after testing several IgG capturing and cleavage conditions, as well as glycan purification conditions (described in the supplemental material). The final workflow allowing the generation and the purification of IgG Fc and Fab fragments from serum is presented in Fig. 2. Briefly, IgG was captured from serum or plasma using anti-IgG-Fc beads. The capturing buffer was then replaced by IdeS digestion buffer and the IdeS protease. After overnight digestion, the Fab fragment was collected in the flowthrough, and the Fc portion in the eluate. A typical SDS-PAGE analysis of the different fractions is depicted in Fig. 2. Importantly, no Fc band was observed in the Fab sample. Protein purity was further assessed using LC-MS/MS analysis after in-solution tryptic digestion of the fractions, which showed only some albumin contamination (supplemental Table S2). Some cross-contamination of Fab peptides in the Fc fraction, and vice versa, was observed. However, MALDI-TOF-MS spectra of the released glycans from the different fractions (total IgG, Fc, and Fab) demonstrated that contamination was only minor, confirming the SDS-PAGE analysis. More specifically, the most abundant Fc glycans (>75% summed relative abundance within the Fc spectra) represented <1% summed relative abundance in the Fab spectra (Figs. 3*B* and 3*C*). Overall, the profile spectra were in good agreement with literature data on IgG glycosylation (3, 14, 23).

Derivatization and HILIC Purification of Released Fab and Fc N-glycans—For high-throughput data gathering, a simple mass spectrometric approach, such as MALDI-TOF-MS, is most convenient. To suppress in-source and metastable

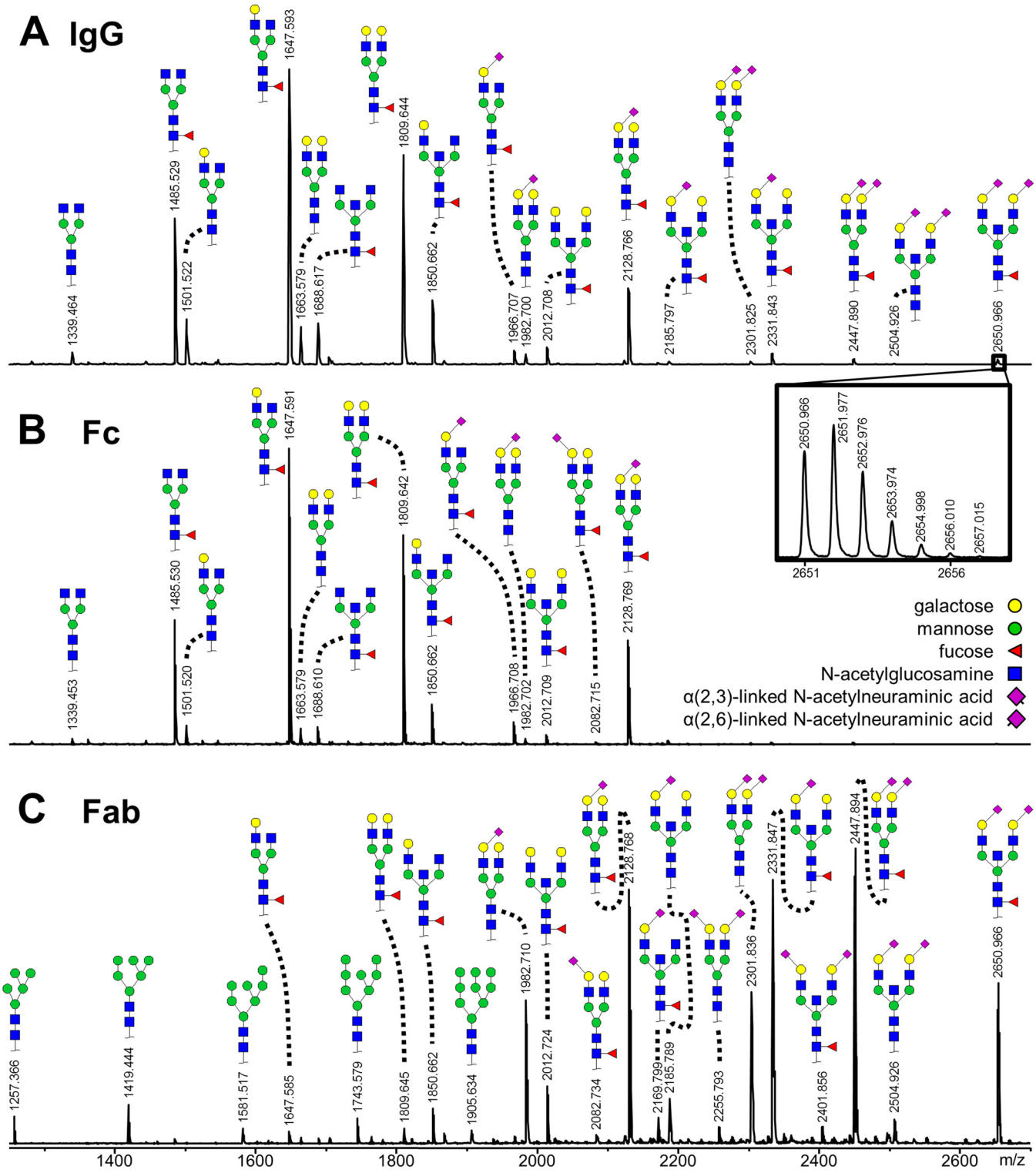

FIG. 3. **Typical IgG, Fc, and Fab mass spectra.** Typical MALDI-TOF-MS spectra obtained for the released glycans of total IgG (*A*), Fc (*B*), and Fab (*C*). The zoomed view shows isotopic resolution even for the low-abundant peaks.

decay of sialylated N-glycans in MALDI-TOF-MS measurements, we performed a derivatization step. The N-glycans were derivatized by ethyl esterification of α2,6-linked sialic acids and lactonization of α2,3-linked sialic acid residues using a recently developed protocol that additionally allows one to differentiate sialic acid linkages (31).

After the derivatization, N-glycan samples were purified via HILIC SPE. To this end, the recently introduced cotton wool

TABLE I
Fc and Fab were differentially glycosylated, as illustrated by the means and S.E. values of glycosylation features of IgG from healthy individuals 26 to 52 weeks after delivery. p values were obtained via Wilcoxon sign-ranked test

	IgG (mean%; S.E.) $n = 28$	Fc (mean%; S.E.) $n = 28$	Fab (mean%; S.E.) $n = 25$	p
Galactosylation	66.59 (1.08)	67.41 (1.19)	94.33 (0.44)	<0.0001
N	78.40 (0.70)	81.16 (0.77)	7.42 (0.53)	<0.0001
S1	18.35 (0.60)	18.23 (0.76)	40.31 (0.72)	<0.0001
S2	3.24 (0.17)	0.61 (0.08)	52.27 (1.08)	<0.0001
Fucosylation	91.90 (0.57)	94.44 (0.39)	69.47 (1.42)	<0.0001
Bisection	12.83 (0.46)	9.84 (0.34)	45.34 (1.38)	<0.0001
High mannose	0.21 (0.01)	0.08 (0.01)	3.60 (0.37)	<0.0001
α2,3-linked sialic acids (%)	0.2 (0.01)	0.1 (0.01)	1.88 (0.10)	<0.0001
α2,6-linked sialic acids (%)	12.3 (0.41)	9.60 (0.38)	70.55 (0.76)	<0.0001

HILIC micro-SPE approach (32) was adjusted to make it less laborious while keeping it compatible with high-sensitivity MALDI-TOF-MS analysis. Whereas in the original method small pieces of cotton wool (approximately 500 μg of cotton wool) are brought into a pipette tip to form a filterless HILIC stationary phase, we here packed small pieces of cotton thread (approximately 180 μg and 3 mm long) into a pipette tip, which made the preparation of the cotton tips easier and faster while maintaining the high yield of the original cotton wool microtips (32). The total time required for preparing the HILIC tips and executing the SPE purification was ~45 min for 96 samples (one plate).

High-throughput Analysis of released Fab and Fc N-glycans—To demonstrate the applicability of the developed method, we subjected aliquots of ethyl esterified glycans from IgG, Fab, and Fc to cotton thread HILIC micro-SPE, spotted with 2,5-dihydroxybenzoic acid matrix, followed by recrystallization with ethanol for optimal MALDI shot-to-shot reproducibility. This MALDI-TOF-MS method was applied on 174 serum samples obtained from 29 healthy women during and after pregnancy, as well as on nine replicates of a standard sample.

Glycans observed for total IgG, Fab, and Fc of human IgG were assigned on the basis of literature knowledge (23, 33), and this glycan list was refined based on species observed in a subset of samples. The final list of detected glycans and their calculated masses are depicted in supplemental Table S1. Glycan compositions and major structural features of the most abundant glycans from Fc and Fab spectra were confirmed using MALDI-TOF/TOF-MS/MS (supplemental Fig. S1).

IgG, Fab, and Fc spectra were internally calibrated, and then glycan signals were extracted and subsequently normalized to a total sum of 100%. Low-quality profiles, as judged by total signal intensity and signal-to-noise ratio, were removed. Two spectra were excluded for IgG, two for Fc, and 24 out of 174 for Fab.

Robustness of the Method—The repeatability of the method was tested using a control serum sample along with the test sera. Inter- and intraplate variation was calculated for the glycans with an average relative abundance of 1% or more over all control samples. In the IgG samples there were nine major glycans, representing >95% of the glycan signal in the spectrum, with average variations of 9% intraplate and 12% interplate. For Fc spectra, seven glycans, representing >95% of the total glycan signal, showed average variations of 12% intraplate and 18% interplate. The Fab spectra contained 11 most abundant signals, representing >93% of the total glycan signal, with average variations of 12% intraplate and 17% interplate. Average relative intensities of all extracted glycans and their standard deviation are presented in supplemental Fig. S2, as are the calculated glycosylation traits. In addition, the relative intensities of the major glycans of IgG, Fc, and Fab and the corresponding relative standard deviations are depicted in supplemental Table S3.

Fc and Fab Are Differentially Glycosylated—Data of the pregnancy time courses were analyzed to reveal glycosylation differences between Fab and Fc, as well as pregnancy-associated changes in Fab glycosylation. For the former purpose, we compared the Fab and Fc glycosylation profiles obtained for the last time point (6 months after delivery), as these samples would hardly be affected by the preceding pregnancy, as we observed in the dataset of a previous study on Fc glycosylation and rheumatoid arthritis (3). Glycosylation patterns were compared after signal extraction and normalization. Levels of galactosylation were on average found to be much higher for Fab (94%) than for Fc (67%, $p < 0.0001$; Table I). Likewise, the levels of sialylation were much higher for Fab than for Fc: monosialylated species were 40% for Fab *versus* 18% for Fc ($p < 0.0001$). For disialylated species, the differences were even more pronounced, with 52% for Fab and less than 1% for Fc ($p < 0.0001$). Additionally, there was a difference in the sialic acid linkages. On Fab, 1.9% α2,3-linked sialylation was observed, whereas only trace amounts (0.1%) of α2,3-linked sialic acids were found in the Fc fraction ($p < 0.0001$). In line with the presence of sialylated glycan species, the percentage of neutral glycans was much lower for Fab (7%) than for Fc (81%; $p < 0.0001$). Levels of bisection were higher for Fab (45%) than for Fc (10%; $p < 0.0001$).

Interestingly, although Fab glycans were high in galactosylation, sialylation, and bisection, they were low in fucosylation relative to Fc (69% *versus* 94%; $p < 0.0001$).

Pregnancy-associated Changes in Fab Glycosylation—In addition to the comparison between Fab and Fc glycosylation, changes in time within the different IgG portions were analyzed. The changes in time of the mean levels of glycosylation traits with pregnancy and after delivery are given in Fig. 4 and Table II, and data distribution is visualized using a boxplot representation in supplemental Fig. S3. Additionally, for all the individual observed glycans, the relative abundances at the different time points are presented in supplemental Fig. S4, and the relative abundances at 6 months after delivery are numerically depicted in supplemental Table S1, along with the standard deviations. The observations presented in Fig. 4 appear similar for total IgG and Fc, although total IgG levels were increased for glycosylation traits that were high on the Fab portion (see, for example, Fig. 4*D*).

First, we looked at changes in IgG Fab and Fc glycosylation with delivery. On the Fab portion, increased levels of monosialylated glycans were detected 6 weeks after delivery (41%) relative to the third trimester of pregnancy (37%; $p < 0.0001$; Fig. 4*C*), at the expense of Fab disialylation (56% to 51%; $p < 0.0002$; Fig. 4*D*). The total percentage of both α2,3- and α2,6-linked sialic acids decreased after delivery for Fab and Fc (Figs. 4*H* and 4*I*). In addition, increases after delivery were observed for fucosylation (67% in the third trimester to 70%; $p < 0.002$; Fig. 4*F*). Notably, bisection showed a rather prominent increase with delivery (from 37% to 45%; $p < 0.0002$; Fig. 4*E*). A decrease was detected within 6 weeks after delivery for Fc galactosylation (77% to 69%; $p < 0.0001$; Fig. 4*A*) and monosialylation (25% to 19%; $p < 0.0001$). The sialic acids were mainly α2,6-linked. Increased levels of α2,3-linked sialic acids were observed on Fab relative to Fc. Neutral Fc glycans were found to be relatively more abundant 6 weeks after delivery (80%) than in the third trimester of pregnancy (75%; $p < 0.0001$; Fig. 4*B*). Fc fucosylation was already high during pregnancy and showed a slight increase with delivery (94% to 95%; $p < 0.0002$). Additionally, the presence of a bisecting GlcNAc on Fc glycans was increased after delivery (10%) relative to the last time point during pregnancy (8%; $p < 0.0001$). Thus, these comparisons established clear and consistent differences in Fab and Fc glycosylation between pregnancy (third trimester) and non-pregnant status (6 weeks after delivery). No major differences were observed between the three post-pregnancy time points (6 weeks, 3 months, and more than 6 months after delivery (Fig. 4)).

Next, we looked at glycosylation changes occurring in the time course of pregnancy. For this, we analyzed changes in IgG Fab and Fc glycosylation between the first and third trimesters of the pregnancy. Regarding the Fab portion, no obvious glycosylation changes were observed, except perhaps for a minor but significant decrease in monosialylated (from 38% in the first trimester to 37% in the third trimester; $p < 0.003$) and bisected glycoforms (39% to 37%; $p < 0.03$), and the percentage of α2,3-linked sialic acid showed a minor increase during pregnancy. In contrast, for the Fc, more pronounced changes in glycosylation were observed. An increase in the level of galactosylation was observed between the first (74%) and third trimesters (77%; $p < 0.0001$). Similarly, an increase in the level of monosialylation was observed when comparing the first (23%) and third trimesters (25%; $p < 0.002$). Glycans on the Fc portion appeared to be less fucosylated in the third trimester (94.1%) than in the first trimester (94.5%; $p < 0.03$). Likewise, neutral glycosylation was decreased in the third trimester (75%) relative to the first (76%; $p < 0.002$). The abundance of high-mannose structures did not change significantly for either Fab or Fc (Fig. 4*G*).

DISCUSSION

Here we present a high-throughput profiling method for analyzing the glycosylation of both the constant and the variable region of polyclonal serum immunoglobulin G in a straightforward workflow. We applied the method to compare Fab and Fc glycosylation profiles of young women and to study pregnancy-associated changes in IgG Fab and Fc glycosylation in the same group. The analysis of Fc released glycans using the method described in this manuscript yielded results that were highly comparable to those previously obtained for the same sample set via LC-MS (3, 24). In addition, this approach for the first time provided high-quality Fab glycosylation data for a clinical cohort.

Glycosylation analysis of the Fab domain of IgG has been performed before, but mainly on monoclonal antibodies (20, 22, 34–37). To our knowledge only a few papers describe analysis of the Fab glycosylation of polyclonal IgG derived from peripheral blood, and only very limited numbers of sera were studied (14, 21, 23), leaving the nature of human polyclonal IgG Fab glycans and their biological variation largely obscure. Additionally, *Sambucus nigra* agglutinin and concanavalin A (ConA) assays provided inconclusive insights into the molecular nature of human Fab glycosylation (16, 26, 38–41). In contrast to these lectin-based assays, the method described in this paper uses mass spectrometric detection of IgG-derived N-glycans and, in combination with an optimized method for the preparation of Fc and Fab portions, provides detailed information on relative abundances, compositions, and major structural features of IgG Fab and Fc N-glycans. Obviously, the mass spectrometric approach for the detection of released glycans is relative by nature, and no absolute quantitation results can be obtained. Furthermore, due to the normalization on total intensity, relative abundances are reported throughout.

We used an innovative on-bead digestion preventing the need for additional purification procedures to obtain separate Fc and Fab samples. The IdeS enzyme has been used before for the generation of Fc and Fab portions and their glycosylation analysis, but mainly on monoclonal antibodies (36, 42,

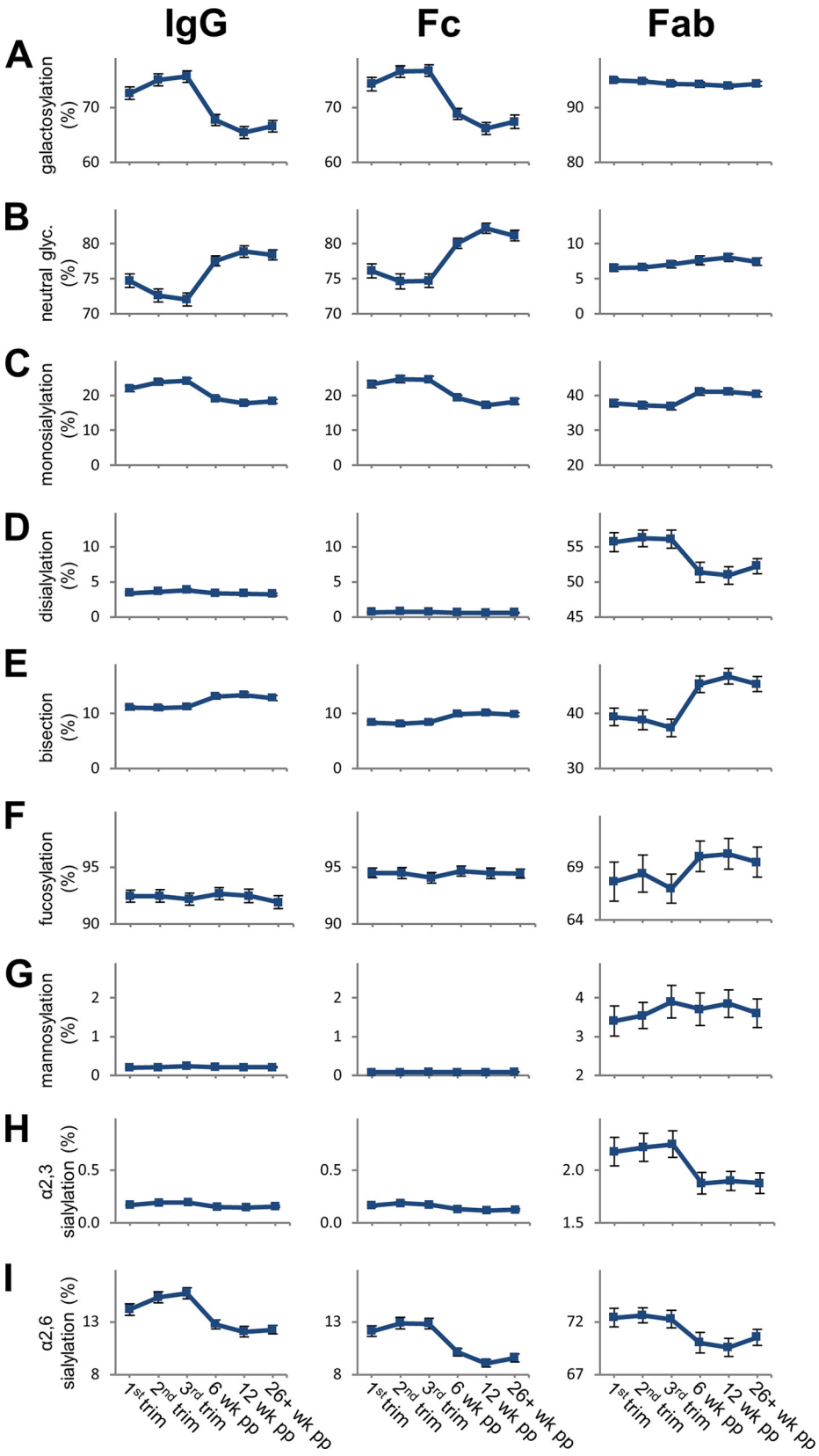

FIG. 4. **Timelines representing glycosylation variation during and after pregnancy.** Various differences in glycosylation between pregnancy and after-delivery time points can be observed for total IgG (*left*), Fc (*middle*), and Fab (*right*) with respect to galactosylation (*A*), neutral (*B*), mono- and disialylated glycans (*C*, *D*), incidence of bisecting GlcNAc (*E*), fucosylation (*F*), the abundance of high-mannose structures (*G*), and α2,3- (*H*) and α2,6-linked (*I*) sialic acids. Error bars represent the standard error of the mean. Abbreviations: trim, trimester of pregnancy; wk, weeks; pp, postpartum.

TABLE II

Glycosylation changes during pregnancy (first versus third trimester) and immediately after delivery (third trimester versus 6 weeks postpartum)

	IgG			Fc			Fab		
	Mean (%)	S.D. (%)	*p* value[a]	Mean (%)	S.D. (%)	*p* value[a]	Mean (%)	S.D. (%)	*p* value[a]
Galactosylation									
trim1	72.60	5.46		74.25	5.83		94.95	2.07	
trim3	75.63	5.75	**<0.0001**	76.68	5.71	**<0.0001**	94.33	2.28	0.1790
6wkpp	67.71	5.40	**<0.0001**	68.83	5.38	**<0.0001**	94.16	2.48	0.3720
Neutral glycosylation									
trim1	74.71	4.65		76.15	4.93		6.54	2.44	
trim3	72.03	5.06	**<0.0001**	74.72	5.26	**0.0015**	7.07	2.60	0.3507
6wkpp	77.53	3.79	**<0.0001**	80.07	3.93	**<0.0001**	7.61	3.01	0.1396
Monosialylation									
trim1	21.88	4.03		23.16	4.92		37.77	4.57	
trim3	24.14	4.40	**<0.0001**	24.56	5.28	**0.0012**	36.83	4.71	**0.0025**
6wkpp	19.10	3.21	**<0.0001**	19.32	3.93	**<0.0001**	40.99	4.70	**<0.0001**
Disialylation									
trim1	3.41	0.99		0.69	0.47		55.69	6.40	
trim3	3.84	1.04	**0.0011**	0.73	0.67	0.6987	56.09	6.55	0.0674
6wkpp	3.37	0.94	**0.0023**	0.61	0.37	0.0817	51.40	6.95	**0.0001**
Fucosylation									
trim1	92.44	2.52		94.49	2.28		67.63	5.84	
trim3	92.19	2.90	0.3044	94.06	2.45	**0.0288**	66.97	7.11	0.1354
6wkpp	92.66	2.87	**0.0017**	94.65	2.32	**0.0001**	70.02	6.90	**0.0017**
Bisecting GlcNAc									
trim1	11.07	2.23		8.33	1.72		39.39	7.32	
trim3	11.21	2.28	0.4300	8.40	1.74	0.9637	37.40	7.98	**0.0206**
6wkpp	13.07	2.52	**<0.0001**	9.88	2.12	**<0.0001**	45.35	7.15	**0.0001**
High mannose									
trim1	0.20	0.04		0.07	0.06		3.40	1.91	
trim3	0.24	0.08	**0.0104**	0.08	0.04	0.1580	3.90	2.14	0.2322
6wkpp	0.22	0.06	**0.0242**	0.08	0.04	0.2563	3.71	2.03	0.8076
α2,3 sialic acid									
trim1	0.17	0.03		0.16	0.07		2.17	0.61	
trim3	0.19	0.04	**0.0002**	0.17	0.05	**0.0323**	2.24	0.65	**0.0276**
6wkpp	0.15	0.03	**<0.0001**	0.13	0.04	**<0.0001**	1.87	0.48	**0.0010**
α2,6 sialic acid									
trim1	14.18	2.66		12.11	2.44		72.40	4.20	
trim3	15.71	2.89	**0.0001**	12.83	2.62	**0.0018**	72.26	4.21	0.7369
6wkpp	12.77	2.22	**<0.0001**	10.14	1.95	**<0.0001**	70.02	4.69	**0.0007**

[a] Wilcoxon sign-ranked test *p* values < 0.05 are highlighted in bold and considered significant. The statistical test was used to make a pairwise comparison of the first and third trimesters (trim1 and trim3, respectively) and of the third trimester *versus* 6 weeks postpartum (6wkpp).

43). IdeS is known to cleave only IgG at a specific cleavage site (29), leaving both Fab and Fc intact. Alternative enzymes come with some disadvantages, like a varying digestion site (44) or multiple digestion sites in the Fc portion (14).

The ethyl esterification of sialic acids used in this study allowed for sensitive detection of glycans using MALDI-TOF-MS in reflectron positive mode (32). This resulted in high-resolution spectra, without the loss of sialic acids that is common in reflectron positive MALDI measurements (45). We registered levels of Fc sialylation similar to those determined via LC-MS (3, 24); without stabilization, sialic acids exhibit low relative abundances in MALDI-TOF-MS experiments (25). In addition, sialic acid ethyl esterification results in linkage-specific mass differences (31). This allowed the facile differentiation of α2,3- and α2,6-linked sialic acids in a high-throughput fashion.

Analysis of our data confirmed previous reports of the presence of high-mannose structures on the Fab portion of IgG (23). The data indicate higher levels of these glycans than observed by Anumula (23). Additionally, we observed drastically lower levels of H3N4F1 and H4N4F1 structures on Fab than reported previously. As these glycans may be largely regarded as Fc markers, this might indicate greater purity of the Fab preparation in our study than in the previous one (23). One possible explanation is that the sequential release of glycans by different enzymes features a less stringent specificity for Fab and Fc than indicated (23).

We analyzed 174 serum samples of 29 individuals covering six time points during and after pregnancy. In this way we were able to observe several changes over time (Fig. 4). Biological variation seemed greater on the Fab portion than on the Fc, as reflected by increased standard error that could not be attributed to technical variation. By applying this method, we demonstrated various changes in Fab glycosylation with pregnancy.

The calculated glycosylation traits show different behaviors for Fc and Fab. For example, although different levels were observed for Fc galactosylation during pregnancy and

6 weeks after pregnancy, this did not occur for Fab galactosylation. Similarly, although to a lesser extent, Fab fucosylation did change after delivery, whereas Fc fucosylation remained at very similar levels throughout. Furthermore, for monosialylation, opposite changes were observed. Monosialylated structures were increased on the Fc portion during pregnancy and decreased after delivery. In contrast, Fab monosialylation was decreased during pregnancy relative to the time points after delivery, which might reflect increased turnover of Fab mono- into disialylated species. However, for both Fab and Fc glycosylation, the level of bisection decreased during pregnancy, and total sialylation increased.

In contrast to the Fc glycosylation, limited information is available with regard to Fab glycosylation function. In fact, most of the data have been obtained recently. Initially it was shown that the anti-inflammatory properties of intravenous immunoglobulins were due to sialylation of the Fc portion (46). However, an increasing body of evidence suggests that the Fab portion is involved (47, 48). Lectins such as Siglecs (sialic acid–binding immunoglobulin-type lectins) and DC-SIGN (dendritic cell-specific intercellular adhesion molecule-3-grabbing non-integrin), recognizing one of the sugar moieties on either one of the IgG portions, may (48–50) or may not (11, 47) be involved in these processes. In addition to the influence of Fab glycans on cellular receptors, the glycans may also be involved in modulating antigen binding and antibody half-life (17, 20).

Increased ConA reactivity during pregnancy has been described in the literature (26, 38, 39). This is generally interpreted as an increase in Fab glycosylated (also called asymmetrical) antibodies, which occurs under the influence of progesterone (38), among other factors. An increase in ConA reactivity *in vitro* has been confirmed by some (27); others observed similar increases in ConA reactivity with low progesterone concentrations, whereas high concentrations resulted in a decrease (51). The increase in ConA reactivity is believed to reflect increased levels of high-mannose glycans only present on the Fab portion, excluding interference from the Fc portion (Asn297), which is known to bear hardly any oligomannosidic glycans (2, 6, 35, 52). However, ConA has also been reported to have affinity for non-bisected glycan structures (41), thereby exhibiting increased binding with decreased levels of bisecting GlcNAc with pregnancy on both Fc and Fab. One may speculate that the glycosylation changes observed in our study were likewise caused by hormonal changes, but more studies are needed to reveal how the cellular glycosylation machinery is regulated by hormones.

In conclusion, we developed a high-throughput method enabling the separate detection of glycans derived from human polyclonal IgG, Fab, and Fc. When this technique was applied to consecutive serum samples from a cohort of pregnant women, it revealed clear differences between Fc and Fab glycosylation of immunoglobulin G. In addition, this technique proved to be suitable for demonstrating pregnancy-associated changes in glycosylation not only for Fc, but also for Fab.

Acknowledgments—We thank Irina Dragan for helping with the sample purity controls, and Hae-Won Uh for advice on the statistical approach.

* This project is funded by the Dutch Arthritis Foundation (NR 10–1-411) and by the European Union's Seventh Framework Program (FP7-Health-F5–2011) under Grant No. 278535 (HighGlycan). Maurice H. J. Selman thanks Hoffmann la Roche for financial support.

S This article contains supplemental material.

‡‡ To whom correspondence should be addressed: Dr. Manfred Wuhrer, PO Box 9600, 2300 RC Leiden, Tel.: 31-0-71-52-66396, E-mail: m.wuhrer@lumc.nl.

REFERENCES

1. Arnold, J. N., Wormald, M. R., Sim, R. B., Rudd, P. M., and Dwek, R. A. (2007) The impact of glycosylation on the biological function and structure of human immunoglobulins. *Annu. Rev. Immunol.* **25,** 21–50
2. Parekh, R. B., Dwek, R. A., Sutton, B. J., Fernandes, D. L., Leung, A., Stanworth, D., Rademacher, T. W., Mizuochi, T., Taniguchi, T., Matsuta, K., Takeuchi, F., Nagano, Y., Miyamoto, T., and Kobata, A. (1985) Association of rheumatoid arthritis and primary osteoarthritis with changes in the glycosylation pattern of total serum IgG. *Nature* **316,** 452–457
3. Bondt, A., Selman, M. H. J., Deelder, A. M., Hazes, J. M. W., Willemsen, S. P., Wuhrer, M., and Dolhain, R. J. E. M. (2013) Association between galactosylation of immunoglobulin G and improvement of rheumatoid arthritis during pregnancy is independent of sialylation. *J. Proteome Res.* **12,** 4522–4531
4. Parekh, R., Roitt, I., Isenberg, D., Dwek, R., and Rademacher, T. (1988) Age-related galactosylation of the N-linked oligosaccharides of human serum IgG. *J. Exp. Med.* **167,** 1731–1736
5. Ruhaak, L. R., Uh, H.-W., Beekman, M., Koeleman, C. A. M., Hokke, C. H., Westendorp, R. G. J., Wuhrer, M., Houwing-Duistermaat, J. J., Slagboom, P. E., and Deelder, A. M. (2010) Decreased levels of bisecting GlcNAc glycoforms of IgG are associated with human longevity. *PLoS One* **5,** e12566
6. Yamada, E., Tsukamoto, Y., Sasaki, R., Yagyu, K., and Takahashi, N. (1997) Structural changes of immunoglobulin G oligosaccharides with age in healthy human serum. *Glycoconj. J.* **14,** 401–405
7. Shields, R. L., Lai, J., Keck, R., O'Connell, L. Y., Hong, K., Meng, Y. G., Weikert, S. H. A., and Presta, L. G. (2002) Lack of fucose on human IgG1 N-linked oligosaccharide improves binding to human FcγRIII and antibody-dependent cellular toxicity. *J. Biol. Chem.* **277,** 26733–26740
8. Ferrara, C., Grau, S., Jäger, C., Sondermann, P., Brünker, P., Waldhauer, I., Hennig, M., Ruf, A., Rufer, A. C., Stihle, M., Umaña, P., and Benz, J. (2011) Unique carbohydrate–carbohydrate interactions are required for high affinity binding between FcγRIII and antibodies lacking core fucose. *Proc. Natl. Acad. Sci. U.S.A.* **108,** 12669–12674
9. Malhotra, R., Wormald, M. R., Rudd, P. M., Fischer, P. B., Dwek, R. A., and Sim, R. B. (1995) Glycosylation changes of IgG associated with rheumatoid arthritis can activate complement via the mannose-binding protein. *Nat. Med.* **1,** 237–243
10. Rademacher, T. W., Williams, P., and Dwek, R. A. (1994) Agalactosyl glycoforms of IgG autoantibodies are pathogenic. *Proc. Natl. Acad. Sci. U.S.A.* **91,** 6123–6127
11. Schwab, I., Seeling, M., Biburger, M., Aschermann, S., Nitschke, L., and Nimmerjahn, F. (2012) B cells and CD22 are dispensable for the immediate antiinflammatory activity of intravenous immunoglobulins in vivo. *Eur. J. Immunol.* **42,** 3302–3309
12. Nesspor, T. C., Raju, T. S., Chin, C. N., Vafa, O., and Brezski, R. J. (2012) Avidity confers FcgammaR binding and immune effector function to aglycosylated immunoglobulin G1. *J. Mol. Recognit.* **25,** 147–154
13. Jung, S. T., Reddy, S. T., Kang, T. H., Borrok, M. J., Sandlie, I., Tucker, P. W., and Georgiou, G. (2010) Aglycosylated IgG variants expressed in bacteria that selectively bind FcgammaRI potentiate tumor cell killing by monocyte-dendritic cells. *Proc. Natl. Acad. Sci. U.S.A.* **107,** 604–609
14. Holland, M., Yagi, H., Takahashi, N., Kato, K., Savage, C. O., Goodall,

D. M., and Jefferis, R. (2006) Differential glycosylation of polyclonal IgG, IgG-Fc and IgG-Fab isolated from the sera of patients with ANCA-associated systemic vasculitis. *Biochim. Biophys. Acta* **1760,** 669–677
15. Stadlmann, J., Pabst, M., and Altmann, F. (2010) Analytical and functional aspects of antibody sialylation. *J. Clin. Immunol.* **30,** 15–19
16. Xu, P.-C., Gou, S.-J., Yang, X.-W., Cui, Z., Jia, X.-Y., Chen, M., and Zhao, M.-H. (2012) Influence of variable domain glycosylation on anti-neutrophil cytoplasmic autoantibodies and anti-glomerular basement membrane autoantibodies. *BMC Immunol.* **13,** 10
17. Coloma, M. J., Trinh, R. K., Martinez, A. R., and Morrison, S. L. (1999) Position effects of variable region carbohydrate on the affinity and in vivo behavior of an anti-(1→6) dextran antibody. *J. Immunol.* **162,** 2162–2170
18. Man Sung, C., Scheinberg, D. A., Avdalovic, N. M., McGraw, K., Vasquez, M., Caron, P. C., and Queen, C. (1993) Genetically engineered deglycosylation of the variable domain increases the affinity of an anti-CD33 monoclonal antibody. *Mol. Immunol.* **30,** 1361–1367
19. Wright, A., Tao, M. H., Kabat, E. A., and Morrison, S. L. (1991) Antibody variable region glycosylation: position effects on antigen binding and carbohydrate structure. *EMBO J.* **10,** 2717–2723
20. Huang, L., Biolsi, S., Bales, K. R., and Kuchibhotla, U. (2006) Impact of variable domain glycosylation on antibody clearance: an LC/MS characterization. *Anal. Biochem.* **349,** 197–207
21. Youings, A., Chang, S. C., Dwek, R. A., and Scragg, I. G. (1996) Site-specific glycosylation of human immunoglobulin G is altered in four rheumatoid arthritis patients. *Biochem. J.* **314,** 621–630
22. Mimura, Y., Ashton, P. R., Takahashi, N., Harvey, D. J., and Jefferis, R. (2007) Contrasting glycosylation profiles between Fab and Fc of a human IgG protein studied by electrospray ionization mass spectrometry. *J. Immunol. Methods* **326,** 116–126
23. Anumula, K. R. (2012) Quantitative glycan profiling of normal human plasma derived immunoglobulin and its fragments Fab and Fc. *J. Immunol. Methods* **382,** 167–176
24. Selman, M. H. J., Derks, R. J. E., Bondt, A., Palmblad, M., Schoenmaker, B., Koeleman, C. A. M., van de Geijn, F. E., Dolhain, R. J. E. M., Deelder, A. M., and Wuhrer, M. (2012) Fc specific IgG glycosylation profiling by robust nano-reverse phase HPLC-MS using a sheath-flow ESI sprayer interface. *J. Proteomics* **75,** 1318–1329
25. van de Geijn, F. E., Wuhrer, M., Selman, M. H., Willemsen, S. P., de Man, Y. A., Deelder, A. M., Hazes, J. M., and Dolhain, R. J. (2009) Immunoglobulin G galactosylation and sialylation are associated with pregnancy-induced improvement of rheumatoid arthritis and the postpartum flare: results from a large prospective cohort study. *Arthritis Res. Ther.* **11,** R193
26. Zenclussen, A. C., Gentile, T., Kortebani, G., Mazzolli, A., and Margni, R. (2001) Asymmetric antibodies and pregnancy. *Am. J. Reprod. Immunol.* **45,** 289–294
27. Prados, M. B., La Blunda, J., Szekeres-Bartho, J., Caramelo, J., and Miranda, S. (2011) Progesterone induces a switch in oligosaccharyltransferase isoform expression: consequences on IgG N-glycosylation. *Immunol. Lett.* **137,** 28–37
28. Tonegawa, S. (1983) Somatic generation of antibody diversity. *Nature* **302,** 575–581
29. von Pawel-Rammingen, U., Johansson, B. P., and Bjorck, L. (2002) IdeS, a novel streptococcal cysteine proteinase with unique specificity for immunoglobulin G. *EMBO J.* **21,** 1607–1615
30. Zauner, G., Hoffmann, M., Rapp, E., Koeleman, C. A. M., Dragan, I., Deelder, A. M., Wuhrer, M., and Hensbergen, P. J. (2012) Glycoproteomic analysis of human fibrinogen reveals novel regions of O-glycosylation. *J. Proteome Res.* **11,** 5804–5814
31. Reiding, K. R., Blank, D., Kuijper, D. M., Deelder, A. M., and Wuhrer, M. (2014) High-throughput profiling of protein N-glycosylation by MALDI-TOF-MS employing linkage-specific sialic acid esterification. *Anal. Chem.*, 2014, **86 (12),** pp 5784–5793
32. Selman, M. H., Hemayatkar, M., Deelder, A. M., and Wuhrer, M. (2011) Cotton HILIC SPE microtips for microscale purification and enrichment of glycans and glycopeptides. *Anal. Chem.* **83,** 2492–2499
33. Takahashi, N., Nakagawa, H., Fujikawa, K., Kawamura, Y., and Tomiya, N. (1995) Three-dimensional elution mapping of pyridylaminated N-linked neutral and sialyl oligosaccharides. *Anal. Biochem.* **226,** 139–146
34. Nallet, S., Fornelli, L., Schmitt, S., Parra, J., Baldi, L., Tsybin, Y. O., and Wurm, F. M. (2012) Glycan variability on a recombinant IgG antibody transiently produced in HEK-293E cells. *Nat. Biotechnol.* **29,** 471–476
35. Stadlmann, J., Pabst, M., Kolarich, D., Kunert, R., and Altmann, F. (2008) Analysis of immunoglobulin glycosylation by LC-ESI-MS of glycopeptides and oligosaccharides. *Proteomics* **8,** 2858–2871
36. Chevreux, G., Tilly, N., and Bihoreau, N. (2011) Fast analysis of recombinant monoclonal antibodies using IdeS proteolytic digestion and electrospray mass spectrometry. *Anal. Biochem.* **415,** 212–214
37. Qian, J., Liu, T., Yang, L., Daus, A., Crowley, R., and Zhou, Q. (2007) Structural characterization of N-linked oligosaccharides on monoclonal antibody cetuximab by the combination of orthogonal matrix-assisted laser desorption/ionization hybrid quadrupole-quadrupole time-of-flight tandem mass spectrometry and sequential enzymatic digestion. *Anal. Biochem.* **364,** 8–18
38. Kelemen, K., Bognar, I., Paal, M., and Szekeres-Bartho, J. (1996) A progesterone-induced protein increases the synthesis of asymmetric antibodies. *Cell. Immunol.* **167,** 129–134
39. Barrientos, G., Fuchs, D., Schröcksnadel, K., Ruecke, M., Garcia, M. G., Klapp, B. F., Raghupathy, R., Miranda, S., Arck, P. C., and Blois, S. M. (2009) Low levels of serum asymmetric antibodies as a marker of threatened pregnancy. *J. Reprod. Immunol.* **79,** 201–210
40. Stadlmann, J., Weber, A., Pabst, M., Anderle, H., Kunert, R. J., Ehrlich, H., Peter Schwarz, H., and Altmann, F. (2009) A close look at human IgG sialylation and subclass distribution after lectin fractionation. *Proteomics* **9,** 4143–4153
41. Taniguchi, T., Mizuochi, T., Beale, M., Dwek, R. A., Rademacher, T. W., and Kobata, A. (1985) Structures of the sugar chains of rabbit immunoglobulin G: occurrence of asparagine-linked sugar chains in Fab fragment. *Biochemistry* **24,** 5551–5557
42. Janin-Bussat, M.-C., Tonini, L., Huillet, C., Colas, O., Klinguer-Hamour, C., Corvaïa, N., and Beck, A. (2013) Cetuximab Fab and Fc N-glycan fast characterization using IdeS digestion and liquid chromatography coupled to electrospray ionization mass spectrometry. In *Glycosylation Engineering of Biopharmaceuticals* (Beck, A., ed), pp. 93–113, Humana Press
43. Ayoub, D., Jabs, W., Resemann, A., Evers, W., Evans, C., Main, L., Baessmann, C., Wagner-Rousset, E., Suckau, D., and Beck, A. (2013) Correct primary structure assessment and extensive glyco-profiling of cetuximab by a combination of intact, middle-up, middle-down and bottom-up ESI and MALDI mass spectrometry techniques. *mAbs* **5,** 699–710
44. Bennett, K. L., Smith, S. V., Truscott, R. J. W., and Sheil, M. M. (1997) Monitoring papain digestion of a monoclonal antibody by electrospray ionization mass spectrometry. *Anal. Biochem.* **245,** 17–27
45. Powell, A. K., and Harvey, D. J. (1996) Stabilization of sialic acids in N-linked oligosaccharides and gangliosides for analysis by positive ion matrix-assisted laser desorption/ionization mass spectrometry. *Rapid Commun. Mass Spectrom.* **10,** 1027–1032
46. Kaneko, Y., Nimmerjahn, F., and Ravetch, J. V. (2006) Anti-inflammatory activity of immunoglobulin G resulting from Fc sialylation. *Science* **313,** 670–673
47. Wiedeman, A. E., Santer, D. M., Yan, W., Miescher, S., Käsermann, F., and Elkon, K. B. (2013) Contrasting mechanisms of interferon-α inhibition by intravenous immunoglobulin after induction by immune complexes versus Toll-like receptor agonists. *Arthritis Rheum.* **65,** 2713–2723
48. Trinath, J., Hegde, P., Sharma, M., Maddur, M. S., Rabin, M., Vallat, J.-M., Magy, L., Balaji, K. N., Kaveri, S. V., and Bayry, J. (2013) Intravenous immunoglobulin expands regulatory T cells via induction of cyclooxygenase-2–dependent prostaglandin E2 in human dendritic cells. *Blood* **122,** 1419–1427
49. Séité, J.-F., Guerrier, T., Cornec, D., Jamin, C., Youinou, P., and Hillion, S. (2011) TLR9 responses of B cells are repressed by intravenous immunoglobulin through the recruitment of phosphatase. *J. Autoimmun.* **37,** 190–197
50. Anthony, R. M., Wermeling, F., Karlsson, M. C., and Ravetch, J. V. (2008) Identification of a receptor required for the anti-inflammatory activity of IVIG. *Proc. Natl. Acad. Sci. U.S.A.* **105,** 19571–19578
51. Canellada, A., Blois, S., Gentile, T., and Margni Idehu, R. A. (2002) In vitro modulation of protective antibody responses by estrogen, progesterone and interleukin-6. *Am. J. Reprod. Immunol.* **48,** 334–343
52. Neue, K., Mormann, M., Peter-Katalinic, J., and Pohlentz, G. (2011) Elucidation of glycoprotein structures by unspecific proteolysis and direct nanoESI mass spectrometric analysis of ZIC-HILIC-enriched glycopeptides. *J. Proteome Res.* **10,** 2248–2260